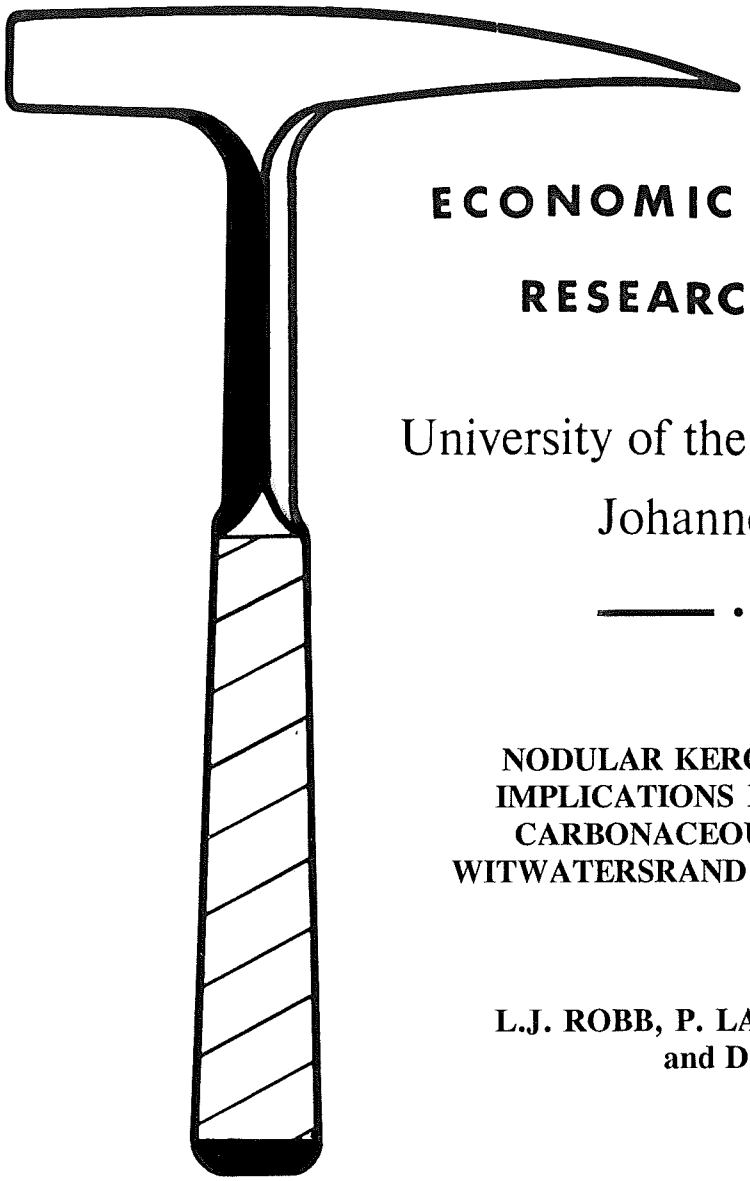

ECONOMIC GEOLOGY

RESEARCH UNIT

University of the Witwatersrand

Johannesburg

NODULAR KEROGEN IN GRANITES: IMPLICATIONS FOR THE ORIGIN OF CARBONACEOUS MATTER IN THE WITWATERSRAND BASIN, SOUTH AFRICA

L.J. ROBB, P. LANDAIS, F.M. MEYER
and D.W. DAVIS

INFORMATION CIRCULAR No. 255

UNIVERSITY OF THE WITWATERSRAND,
JOHANNESBURG

NODULAR KEROGEN IN GRANITES: IMPLICATIONS FOR THE ORIGIN OF CARBONACEOUS MATTER IN THE WITWATERSRAND BASIN, SOUTH AFRICA

by

L.J. Robb,[1] P. Landais,[2] F.M. Meyer[1] and D.W. Davis[3]
([1] *Department of Geology, University of the Witwatersrand, Johannesburg, South Africa*
[2] *CREGU et CNRS, Vandoeuvre-lès-Nancy, France*
[3] *Jack Satterley Geochronology Laboratory, Royal Ontario Museum, Canada)*

ECONOMIC GEOLOGY RESEARCH UNIT
INFORMATION CIRCULAR No. 255

September, 1992

NODULAR KEROGENS IN GRANITES: IMPLICATIONS FOR THE ORIGIN OF CARBONACEOUS MATTER IN THE WITWATERSRAND BASIN, SOUTH AFRICA

ABSTRACT

Nodules of kerogen have been observed in several Archaean peraluminous granites adjoining the gold- and uranium-bearing Witwatersrand Basin. The kerogen usually replaces uraninite or uranothorite in the granite and is paragenetically late. It shows many similarities to kerogen seams and nodules associated with the conglomerate horizons in the Witwatersrand Basin, including composition, maturation, intimate association with uraninite, and a late paragenesis. U-Pb isotope ratios for granite-hosted and Witwatersrand kerogens define a single, albeit somewhat diffuse, Pb-loss discordia suggesting an upper intercept age of circa 2300 Ma. Raman spectroscopy indicates that granite-hosted kerogen is more highly ordered than Witwatersrand seam kerogen, indicating that combined thermal and radiolytic effects have influenced the fixation, aromaticity, structure and composition of the carbonaceous matter.

A model is presented which links the granitoid- and sediment-hosted kerogen to a single event of oil production in the Witwatersrand Basin at circa 2300 Ma ago. Light hydrocarbons migrated through the sediments and into underlying/adjacent granitic rocks, undergoing polymerization and fixation in response to radiation accompanying the presence of high-uranium phases.

_____oOo_____

NODULAR KEROGENS IN GRANITES: IMPLICATIONS FOR THE ORIGIN OF CARBONACEOUS MATTER IN THE WITWATERSRAND BASIN, SOUTH AFRICA

INTRODUCTION

The existence of carbon polymorphs in igneous rocks is common-place and in the case of diamond the origin of the carbon is deep-seated. Kimberlites, as well as carbonatites and nepheline syenites, also commonly contain nodular graphite and in such cases a high P-T origin is again considered appropriate (Gellatly, 1966). Lower temperature, hydrothermal graphite is also often reported and is believed to be associated with circulation of CO_2-CH_4-rich fluids during events of regional metamorphism (Rumble *et al.*, 1986). By contrast, the existence of hydrocarbons in igneous rocks is both rare and unusual, and since there is a tendency for hydrogen-carbon bonds to dissociate at even moderate geological temperatures, their presence is an indication of later, superimposed phenomena.

Kerogen is an important, but volumetrically minor, component of the Archaean Witwatersrand Basin, where it is hosted largely in conglomerate "reefs" as thin (generally < 1 cm thick) seams or nodules. It is commonly associated with high values of gold and uranium. The origin of Witwatersrand kerogen is contentious, and contrasting hypotheses for a syngenetic algal residue (Hallbauer, 1975) and an epigenetic, radiolytically polymerized hydrocarbon-rich fluid (Schidlowski, 1981) have been mooted. Investigations of hydrothermally altered Archaean granites adjoining the Witwatersrand Basin have also revealed the presence of kerogen nodules, usually associated with uraninite/uranothorite (Hallbauer, 1984; Robb and Meyer, 1990; Robb *et al.*, 1990). The present paper describes the nature and occurrence of granite-hosted kerogen from several localities around the basin and makes suggestions regarding their origin and relationship to the Witwatersrand kerogen.

GRANITIC HOST ROCKS

Kerogen nodules have been observed in at least five localities in and around the limits of the contiguous Witwatersrand Basin (Figure 1). The granites which host the nodules are high-SiO_2 varieties, weak-to-moderately peraluminous (peraluminous index = 1,01-1,57) and characterized by adamellitic and granitic (*sensu stricto*) compositions (Table 1). They also exhibit low-CaO contents (< 1%) and contain a high-U phase which is either uraninite or uranothorite (Table 1).

Leucogranite intersected in borehole N4 (Figure 1) is characterized by intense deuteric alteration (propylitic and phyllic) together with minor albitization and quartz-carbonate-sulphide veining (Klemd and Hallbauer, 1987; Robb and Meyer, 1987). The age of the granite is unknown but since it is overlain by a Ventersdorp-type succession it must be older than 2714 Ma (Armstrong *et al.*, 1991). Granites in the Hartbeesfontein area (intersected in boreholes DHF9 and DRH 10) comprise highly siliceous, garnet-bearing, leucogranitoids of adamellitic composition. This suite of granites is characterized by a distinctive greisen style of alteration (Robb and Meyer, 1990; Robb *et al.*, 1990) marked by the development of zones of coarse quartz + muscovite, intense albitization and quartz-chlorite-carbonate-sulphide veins. Greisenized samples exhibit LREE depletion, low Th/U ratios (< 1) and

NODULAR KEROGENS IN GRANITES: IMPLICATIONS FOR THE ORIGIN OF CARBONACEOUS MATTER IN THE WITWATERSRAND BASIN, SOUTH AFRICA

CONTENTS

_____oOo_____

Published by the Economic Geology Research Unit,
Department of Geology,
University of the Witwatersrand,
1 Jan Smuts Avenue,
Johannesburg 2001,
South Africa

ISBN 1 86838 032 7

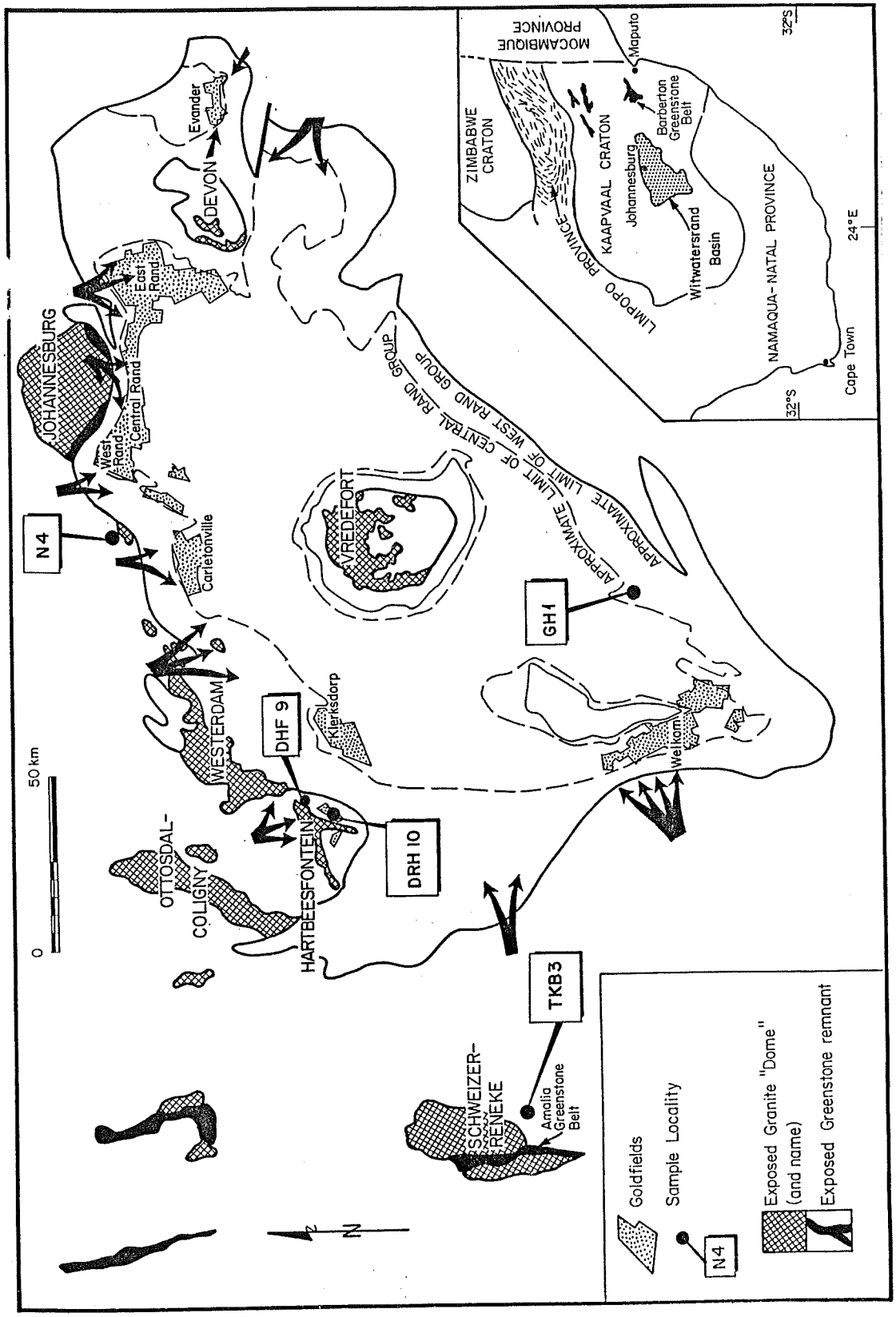

Figure 1: Locality map showing outline of the Witwatersrand Basin and position of granite samples from which kerogen nodules have been obtained.

TABLE 1
MAJOR AND TRACE ELEMENT ANALYSES: GRANITES, KEROGEN AND URANIUM PHASE

		GH1	TKB3 (120)	DHF9 (651)	DRH10 (2783)	N4	TKB3 (kerogen)	GH1 (urano-thorite)
	SiO_2	73.02	70.70	73.90	75.70	72.69		8.66
	TiO_2	.04	.03	.15	.18	.21		1.08
	Al_2O_3	14.11	14.7	14.74	13.40	14.00		.67
wt. %	Fe_2O_3	1.13	1.62	.86	1.14	1.90		.20
	MnO	.03	.01	.07	.02	.01		
	MgO	.16	1.7	.29	.57	.50		
	CaO	.97	2.38	.98	.53	.66		1.18
	Na_2O	4.11	.10	5.40	4.40	3.80		
	K_2O	5.58	5.85	2.46	2.55	4.74		
	P_2O_5	.01	.02	.02	.01	.09		.38
	L.O.I.	.85	4.20	.85	.86	.97		
	TOTALS	100.01	101.30	99.73	99.36	99.48		61.40
	Rb	268	231	90	158	143		
	Sr	184	40	176	117	129	197	
	Ba	485	421	214	424		1802	
	Zr	215	168	224				
	La	51.8	32.9	36.3	32.3		201	1400
	Ce	95.7	70.2	75.2	35.9		607	5500
	Nd	25.4	31.4	27.4	11.4		483	4700
ppm	Sm	4.93	4.44	6.48	1.80		187	2200
	Eu	.85	.89	2.28	.91		42.8	45
	Tb	.76	1.33	1.49	.28		77.5	
	Yb	1.98	3.53	4.90	.51		215	6000
	Lu	.39	.61	.89	.07		26.8	2000
	U	11.1	33.8	10.2	2.3		6040	11.87%
	Th	41.9	26.7	13.8	3.6		2425	20.24%
ppb	Au	.7	3.5	4.1	.5		890	

uranium contents up to 24 ppm. The age of the DHF9 granite, which is unconformably overlain by the 3074 Ma Dominion Group (Armstrong *et al.*, 1991), is 3174 + 9/-7 Ma (Robb et al., 1992).

Adamellites from the Schweizer-Reneke area (Figure 1) exhibit moderate deuteric alteration at surface, but also give rise to Au-enriched (100 ppb) quartz-microcline-chlorite-rutile-sulphide veins. The adamellite is overlain by mid-Ventersdorp Supergroup sediments and near the contact the granitoid is strongly altered and carbonated, causing depleted Na_2O and Sr contents and high loss-on-ignition (TKB3 (120), Table 1). In this zone, late fine-grained quartz veinlets represent fluid conduits which have introduced pyrite, chalcopyrite and kerogen nodules. The age of the TKB3 granite, which is overlain by 2714 Ma old (Armstrong et al., 1991) Ventersdorp sediments, is 2880 $\pm$ 2 Ma old (Robb *et al.*, 1992).

Locality GH1 is the only one where granite is directly overlain by Witwatersrand sediments (Figure 1). The basement material here is a low-CaO, leucocratic adamellite which is characterized by an accessory mineral suite dominated by monazite and uranothorite (Table 1). Uranium contents in this rock vary between 6-116 ppm. Occasional quartz-chlorite-carbonate-sulphide veins occur within the granite. The granite in borehole GH1 has been dated at 3101 $\pm$ 2 Ma (Robb *et al.*, 1992).

KEROGEN NODULES

Petrographic Characteristics

Kerogen occurs as discrete nodules or nodular stringers with diameters ranging from 0,4-4 mm. In many cases the kerogen is demonstrably associated with uraninite or uranothorite and in such situations clearly replaces the latter. In sample DHF9 uraninite, chalcopyrite and pyrite occur within a hydrothermal vein, with the uraninite having been selectively replaced by kerogen (Figure 2 a, b). In GH1, uranothorite is progressively replaced by kerogen, which appears to have permeated individual grains along crystallographic axes. Even where there is no observable association with a discrete high-U phase the kerogen is always associated with very high U contents (up to ~ 2500 ppm; Table 1).

Kerogen nodules are also demonstrably late in terms of the paragenetic sequence of alteration in the granites. In GH1, kerogen clearly replaces euhedral uranothorite which appears to have crystallized as a primary accessory phase together with monazite. In DHF9 a greisen-type alteration is believed to have been early sub-solidus in origin, as suggested by U-Pb age determinations on hydrothermal rutile (Robb *et al.*, 1992). Circulation of hydrocarbons post-dated this event, replacing uraninite that probably formed during greisening. In sample DRH 10 vein-like stringers of kerogen are concentrated along micro-fractures and also within veins formed during greisening, suggesting that late hydrocarbon-bearing fluids took advantage of pre-existing hydrothermal conduits. In sample N4, however, kerogen nodules are marked by an aureole of fibrous mica which presumably formed subsequent to agglutination of the hydrocarbon. Samples from the TKB3 borehole locality have large (3-4 mm diameter) kerogen nodules concentrated within a zone at the

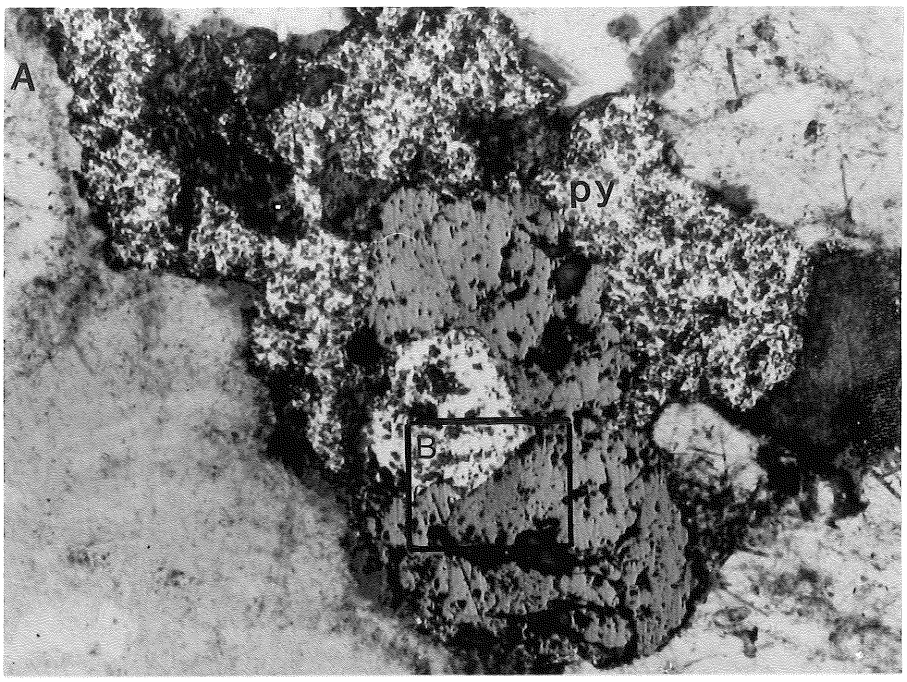

Figure 2: a). Kerogen replacing uraninite in a quartz-chlorite-rutile-chalcopyrite-pyrite-carbonate veinlet from granite DHF9. Width of field of view = 1mm.

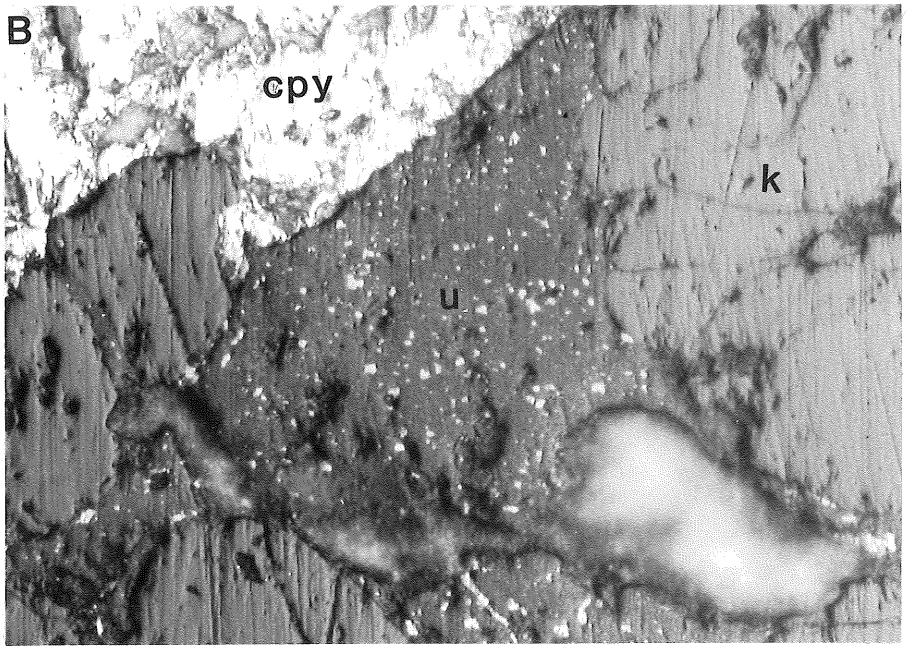

Figure 2: b). Enlarged view of boxed area in Figure 2a. Kerogen (k) replaces uraninite (u) and, to a lesser extent, chalcopyrite (cpy).

interface between argillitized granitic basement and overlying mid-Ventersdorp sediments suggesting that hydrocarbon-bearing fluids might have been flushed along this unconformity in post-Ventersdorp times (i.e. < 2700 Ma ago).

Chemical Characteristics

No major element (C, H, O) analyses of granite-hosted kerogen nodules are available since the volume of material available for analysis is very small. However, granite-hosted kerogen is very similar to Witwatersrand kerogens in terms of rank and petrographic appearance, as well as minor element content (see later and Hallbauer *et al.*, 1986). Witwatersrand kerogens vary in composition and typical ranges are C (30-80%), H (1,5-4,0%) and O (2,3-4,1%) (Hallbauer, 1986; Landais *et al.*, 1990b). Hallbauer (1986; 1991) distinguished geochemically between carbon seams and nodular kerogen in Witwatersrand conglomerate 'reefs' and argued on the basis of differences in trace element content that the former represent syngenetic relictual algal mats while the latter are more akin to the granite-hosted nodules and have an hydrothermal origin. Hallbauer *et al.* (1986) maintained that granite hosted nodules are typically enriched in Na, Ca, Cr, Ni, Cu and Co, but depleted in Sr, Ba, Zn, Ag, Au and Cd relative to Witwatersrand seam kerogen.

In the present study INAA analyses of rare earth elements (REE) are compared in Figure 3. Chondrite normalized REE distribution for host granitoids generally exhibit L-shaped patterns, while U and Th content are enriched relative to crustal abundances (Figure 5). A kerogen nodule (from TKB3) is markedly enriched in total REE content relative to its host granite and is characterized by HREE enrichment and a negative Eu anomaly. Such features are unlikely to have been inherited from the host rock. For comparison, uranothorite from GH1 also shows high total REE content, a pronounced negative Eu anomaly, and HREE enrichment, features that are similar, but more emphatic, than those of the kerogen nodule. It is suggested that the REE pattern of the kerogen nodules derives its signature from the uranium minerals it replaces. Although there is no REE data available for uraninite, either from the sediments or from granites surrounding the basin, analyses of uraninite grains from the Huronian deposits in Canada as well as other uranium ore-deposit types also show high concentrations of total REE, heavy REE enrichments, and pronounced negative Eu anomalies (Fryer and Taylor, 1987).

REE patterns from Witwatersrand seam kerogen show a wide range of abundances, but all have shapes that are similar, and overlap with, the granite-hosted kerogen (Figure 3). Au, U and Th contents tend to be much higher in conglomerate-hosted than in granite-hosted kerogen and this reflects the high degrees of enrichment of these elements in the reefs.

Isotopic Characteristics

Carbon isotope studies of Witwatersrand kerogen concur in identifying the source of carbon as biogenic. Hoefs and Schidlowski (1967) reported $\delta\ ^{13}C$ values for kerogen from several reefs varying between -22,4 and -32,8‰, while a more comprehensive study of five

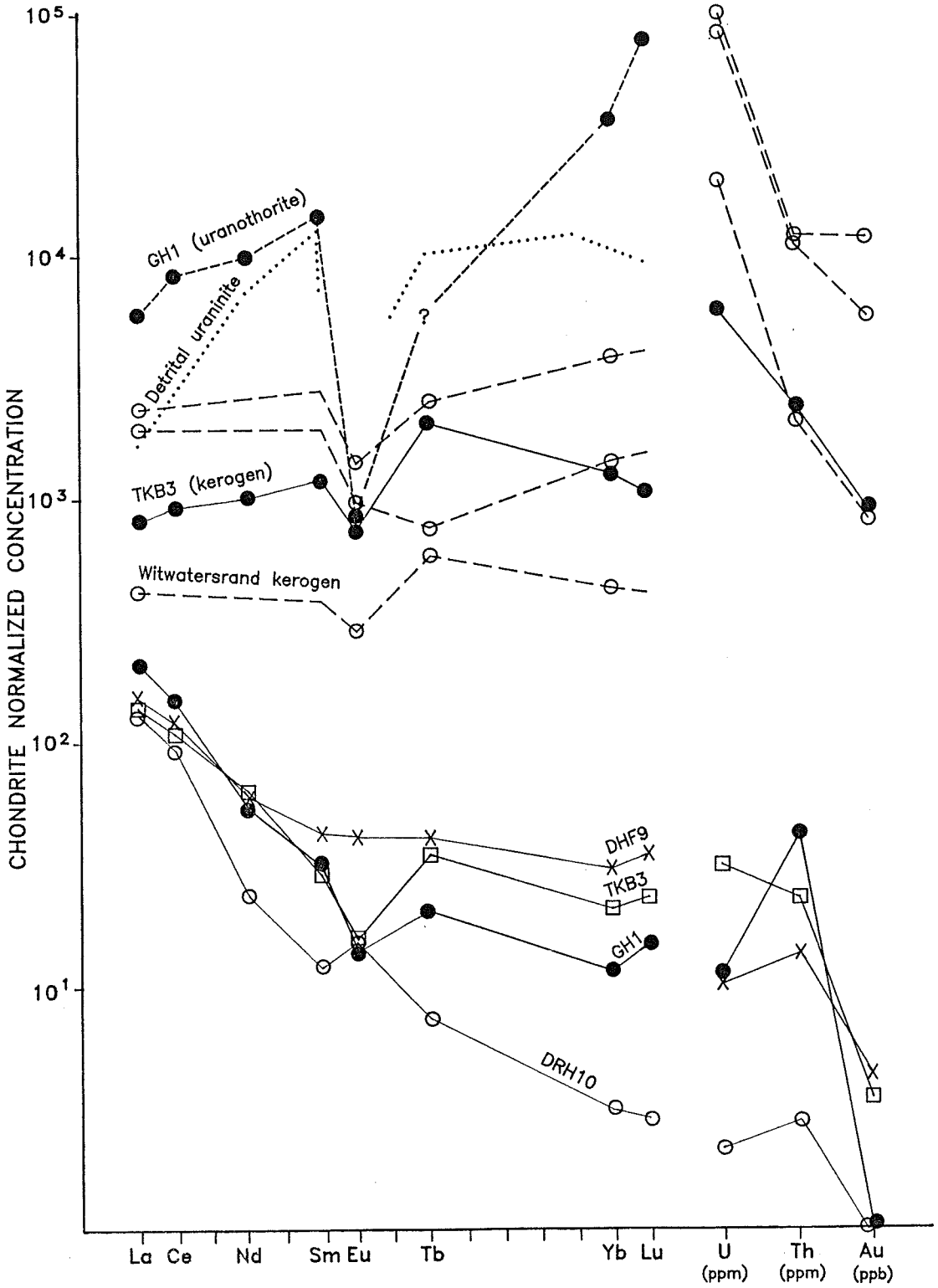

Figure 3: Chondrite normalized REE concentrations and absolute abundances of U, Th and Au for host granitoids. Also shown are Witwatersrand kerogen seams (dashed lines; data from Zumberge et al., 1978), granitoid-hosted kerogen (TKB3) and uranothorite (GH1) and detrital uraninite from the Elliot Lake deposits (dotted line; data from Roscoe, 1969).

different reefs by Förster (1989) presented results showing $\delta\ ^{13}C$ ranging between -25.3±4.8 and -34.0±2.7‰. These ranges point to a biogenic derivation for the source material of the kerogen. The magnitude of the heavy carbon isotope depletion is considered to be more consistent with a generic relationship to oil than to coal products (Hoefs and Schidlowski, 1967). Analysis of a single kerogen nodule from TKB3 yielded a $\delta\ ^{13}C$ value of -36,3‰ indicating that this carbon was most probably derived from the same type of source material as that for the sediment hosted kerogen. It is pertinent to note, however, that the granitoid hosted kerogen is somewhat depleted in ^{12}C compared to typical reef kerogen. Eakin (1989) has demonstrated that heavier $\delta^{13}C$ values are associated with increasing uranium content and this may account for the shift towards lighter isotopic fractions in the granites where uranium contents are considerably lower than in the conglomeratic reefs. Another cause of this fractionation effect may be related to possible differences in the nature of hydrocarbons percolating into the granitoid basement relative to those migrating within the sedimentary pile. Gases formed during hydrocarbon maturation will incorporate more ^{12}C since ^{12}C - ^{12}C bonds are less stable than ^{13}C - ^{12}C bonds (Waples, 1982). Hence, lighter $\delta^{13}C$ values will characterize volatile fractions that migrate further than heavier, less mobile liquid fractions.

U-Pb isotopic analyses of kerogen separated from the Vaal and Carbon Leader Reefs (Allsopp *et al.*, 1986) yielded an upper intercept age of 2320 ± 50 Ma. Kerogen nodules extracted from three samples of peraluminous granite adjoining the Witwatersrand Basin have been analysed in the present study (Table 2) and are plotted together with the Witwatersrand reef data in Figure 4. The three granite-hosted kerogen points define a trend that straddles, and is effectively colinear with, the Witwatersrand kerogen data points; together the data define an upper intercept age of 2267 + 86/-77 Ma.

The interpretation of the U-Pb isotopic data of Figure 4 is equivocal. Allsopp *et al.* (1986) pointed out that the Witwatersrand kerogen data did not conform with either simple episodic or diffusional Pb-loss models and that migration of intermediate daughter products of the U-Pb decay series might have affected the ratios of stable daughter isotope products. However, given that several of the points from both data sets are near concordant, and that carbonaceous matter has been shown to act as a very efficient containment medium for fissiogenic products (Nagy *et al.*, 1991), it is also conceivable that the upper intercept reflects the time that the U-Pb isotopic systems were set in the kerogen of both data sets. This might imply, therefore, that the kerogen within both its sedimentary and igneous host rocks was deposited circa 2300 Ma ago, some 400 Ma after cessation of Witwatersrand Basin sedimentation. This implies that hydrocarbon circulation within the basin could not have been an early diagenetic phenomenon, but must have taken place during a much later discrete event when rock porosity (but not necessarily permeability) was greatly reduced.

Although the absolute chronological significance of the U-Pb isotopic data is contentious, it is apparent that the granite- and sediment-hosted kerogen exhibit similar patterns of U-Pb isotopic evolution. This suggests that, not only was the ultimate source of carbon similar (as suggested by the carbon isotopic data), but that the kerogen fixation in both host rock types was coeval and, possibly, controlled by the same processes.

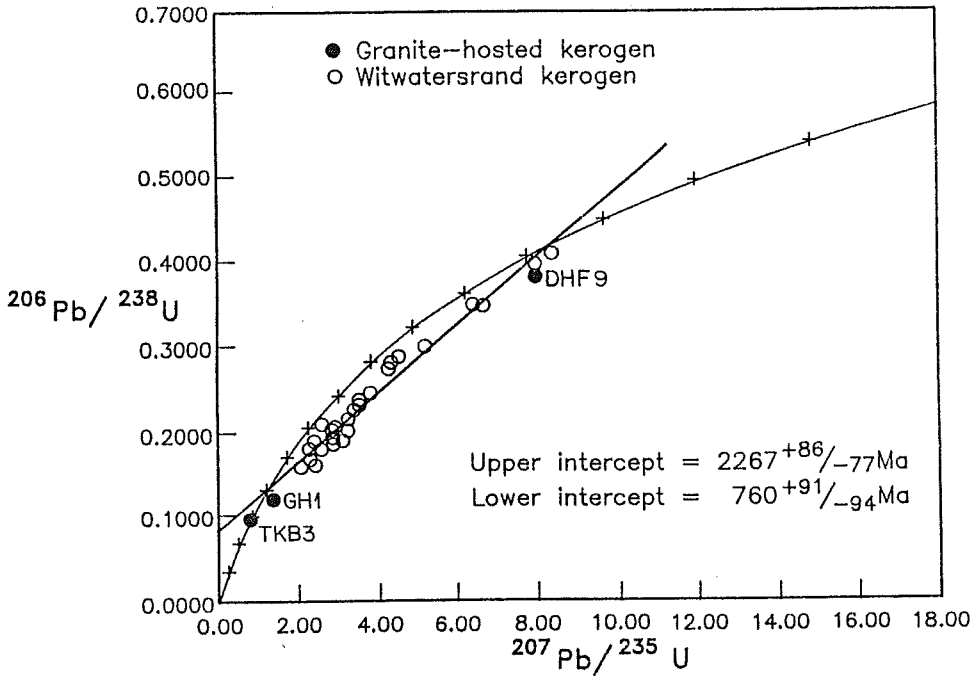

Figure 4: Concordia plot of $^{206}Pb/^{238}U$ versus $^{207}Pb/^{235}U$ for Witwatersrand kerogen (data from Allsopp et al., 1986) and three samples of granitoid-hosted kerogen. Regression of data was carried out using the procedures of Eglington and Harmer, 1991).

TABLE 2
U-Pb AND CARBON ISOTOPIC DATA

	DHF9(651)	TKB3(120)	GH1
Weight (mg)	0.04	.05	.05
U (ppm)	1050	10700	400000
Pb common (pg)	1542	320	39160
Th/U		.29	.17
$^{207}Pb/^{204}Pb$	114.3	561	332
$^{206}Pb/^{238}U$	.38061	.09187	.11786
$^{207}Pb/^{235}U$	7.953	.7030	1.356
$^{207}Pb/^{206}Pb$	.15127	.05570	.08376
% discordance	14.1	-32.0	46.3
AGE (Ma)	2363.4±4.1	432.4±2.6	1280.1±1.6
$\delta^{13}C$		-36.3‰	

Raman Spectral Characteristics

Micro-Raman and Fourier Transformed Infra-Red Spectroscopy have been successfully utilized to obtain structural information on natural kerogens, particularly where it has been affected by proximity to uranium mineralization (Landais *et al.*, 1990a, b; Rochdi and Landais, 1991; Wang *et al.*, 1989). Raman studies of graphite from the Athabaskan unconformity-related uranium deposits show a progressive structural disorganization as the ore-body and its associated alteration halo is approached (Wang *et al.*, 1989), while Witwatersrand kerogens exhibit complex structural re-arrangement as a function of uranium content and proximity to α-radiation damaged halos around individual uraninite grains within the kerogen (Landais *et al.*, 1990a, b).

Micro-Raman analyses of Witwatersrand kerogens reveal two prominent spectral bands at ≈ 1600 cm^{-1} (an E2g2 Raman mode attributed to C-C vibrations) and ≈ 1350 cm^{-1} (which is a defect band which becomes more pronounced with progressive disorganization-alteration). The intensity ratio (I 1600/I 1350) of these two peaks can be determined as a measure of structural organization of the hydrocarbon molecule, and compared to the half-height width (L 1600) of the predominant (1600 cm^{-1}) peak, which is broadly proportional to the uranium content of the carbonaceous matter (Landais *et al.*, 1990a). A plot of I 1600/I 1350 versus L 1600 for granite-hosted kerogen nodules shows that the peak intensity ratio is markedly higher than for both kerogen seams and nodules from Witwatersrand reefs (Figure 5). This implies that the granite-hosted kerogen comprises a hydrocarbon molecule that is structurally better organized than the sediment-hosted kerogen, a feature that may reflect the smaller proportion of kerogen relative to replaced uraninite/uranothorite in the granitic host rock. It is interesting to note that micro-Raman spectra from within the α-radiation damaged halos immediately surrounding uraninite grains from Witwatersrand seam kerogens also display enhanced I 1600/I 1350 ratios and improved organizational structure relative to kerogens away from discrete uraninite particles. These results imply that radiolytic polymerization is the mechanism which influences the molecular structure of kerogen, and is probably the main cause of hydrocarbon fixation in both the Witwatersrand sediments and adjoining peraluminous granites.

TIMING OF ORGANIC MATURATION IN THE WITWATERSRAND BASIN

The time that elapses between sedimentation and oil production may be relatively short (10 - 25 Ma) for orogenically active basins where rapid sedimentation rates prevail, or a much lengthier period (100 - 400 Ma) where basins evolved in stable cratonic or platformal environments (Tissot and Welte, 1978). Computer models which employ burial histories, geothermal gradients, and hydrocarbon maturation activation energies have been used to quantify the kinetic effects of oil and gas production in sedimentary basins (Landais *et al.*, 1990a). In the scenario depicted in Figure 6, where the Witwatersrand sediments are progressively loaded by overlying sequences at 2700 Ma (Ventersdorp Supergroup), at 2500 Ma (Malmani Group) and at 2200 Ma (Pretoria Group), and where a geothermal gradient of 35°C.km^{-1} applies, as suggested by metamorphic studies (Wallmach and Meyer, 1990), computer modelling indicates that the principal period of oil generation would have occurred some 250 Ma after termination of sedimentation. Given that the geothermal gradient

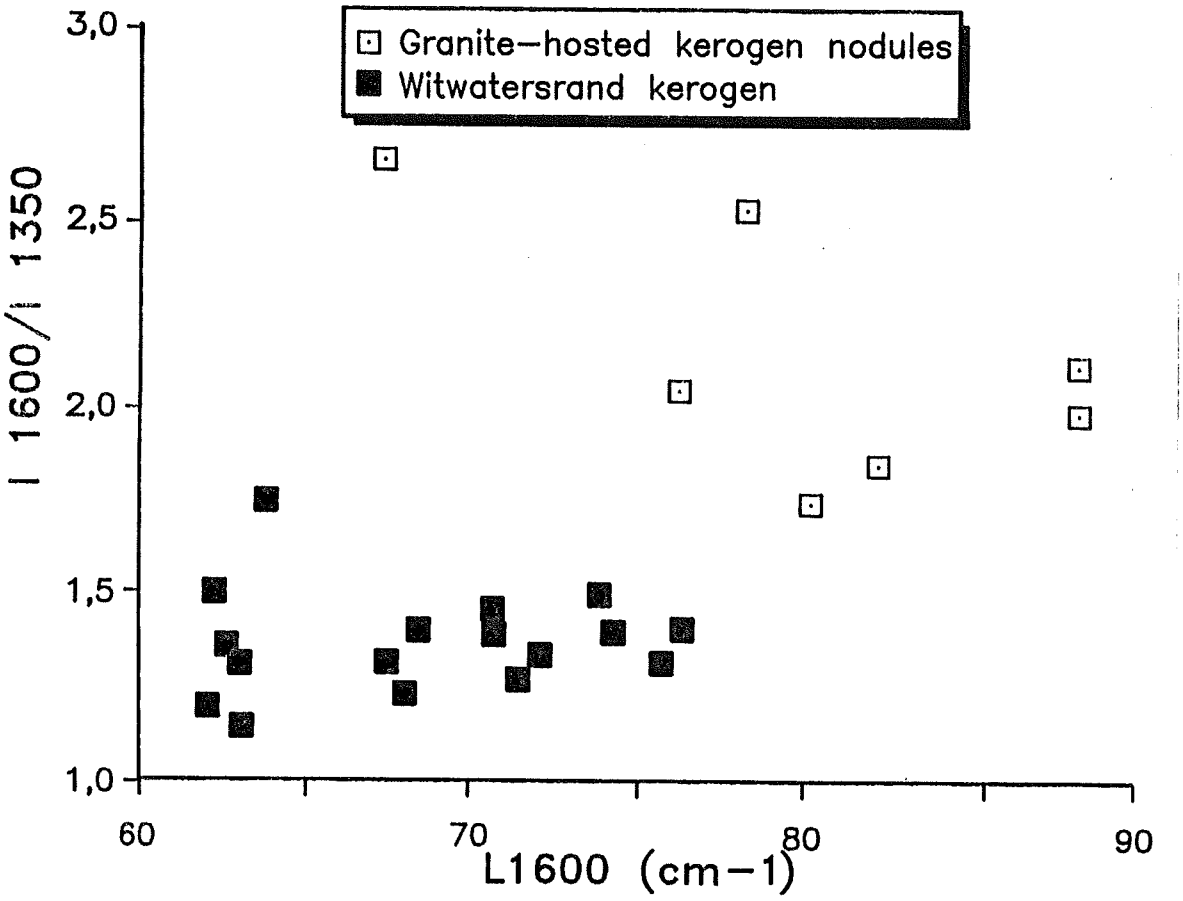

Figure 5: Plot of peak intensity ratios (I 1600/I 1350) versus ½-height width of the dominant peak (L 1600) for Witwatersrand kerogen seams and for granitoid-hosted kerogen nodules.

utilized in this calculation probably applied only during the peak of prograde metamorphism (during the Bushveld event at 2050 Ma ?) and that lower gradients probably existed prior to this event, it is evident that oil production could have occurred even later, and possibly several hundred million years after cessation of sedimentation, as suggested by the Pb isotopic data. If detailed P-T-t studies in the future reveal that the Witwatersrand sediments evolved through the oil window prior to the peak of metamorphism then it is still possible that low molecular weight hydrocarbons (i.e. gases and gasolines) persisted long after the peak of oil production.

DISCUSSION AND CONCLUSIONS

Kerogen nodules in peraluminous granites adjoining the Witwatersrand Basin appear to be genetically linked to kerogen within the sediments themselves. Striking similarities exist in terms of petrographic characteristics, composition, stable and radiogenic isotope characteristics, and in the intimate relationships between kerogen and a uranium phase. In

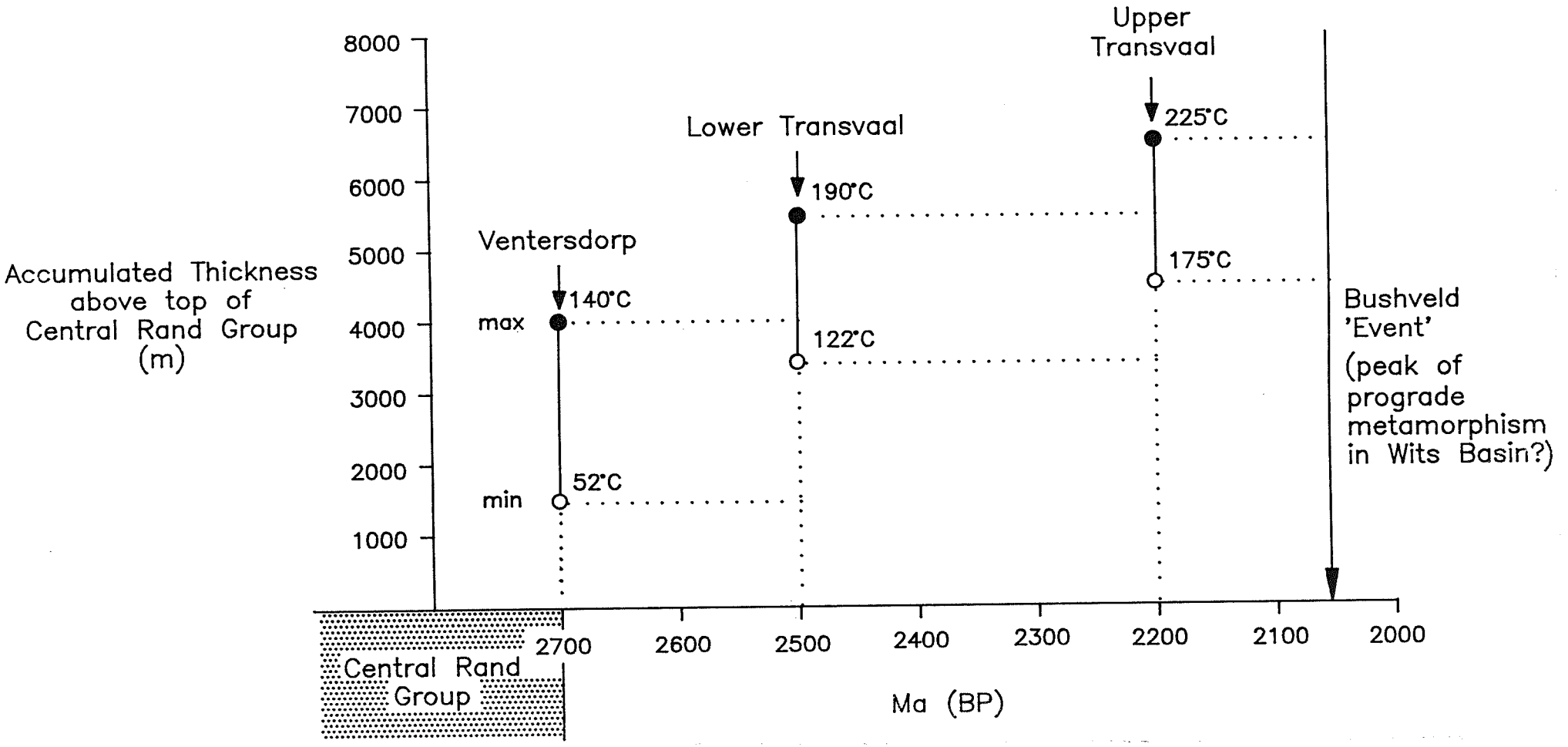

Figure 6: Schematic temperature - time profile showing loading of the Witwatersrand Basin subsequent to its deposition. The age of Ventersdorp Supergroup deposition (c. 2700 Ma) is after Armstrong et al. (1991); lower Transvaal Sequence deposition (c. 2500 Ma) is after Jahn et al. (1990); and upper Transvaal Sequence deposition (c. 2200 Ma) is after Burger and Coertze (1974).

both sediments and granites, kerogen is paragenetically late and in most cases appears to replace, or accumulate around, uraninite or uranothorite. In the Witwatersrand conglomerates kerogen post-dates authigenic pyrite and pyrrhotite veinlets (Landais *et al.*, 1990b) and often appears to have been formed along pre-existing fractures or fluid conduits. Carbon isotope signatures are light and suggest that the source of carbon in both cases was biogenic, and probably derived from the sedimentary pile by organic degradation. U-Pb isotope analysis indicates that both the granite- and sediment-hosted carbonaceous matter was fixed at the same time and, consequently, record similar patterns of U-Pb isotopic evolution that appear to have commenced long after ($\sim$ 400 Ma) the cessation of sedimentation. The structure of the hydrocarbon material is largely influenced by the effects of irradiation and its REE contents appear to reflect a pattern derived from the material (i.e. largely uraninite) which it is replacing.

If it is assumed that both the sediment- and granite-hosted kerogen is genetically linked then any model for the origin and formation of the kerogen occurrences would, of necessity, require the presence of a hydrocarbon-bearing aqueous solution as the transporting medium. Although it is widely believed that the kerogen seams in the Witwatersrand Basin represent *in sutu* remnants of preserved algal/fungal residue (Hallbauer, 1975), the view is adopted here that they are more likely to represent the radiolytically polymerized products of hydrocarbon-bearing solutions passing through the conglomerates (Schidlowski, 1981; Landais *et al.*, in prep.). It is suggested that the principal period of liquid hydrocarbon generation (catagenesis) in the Witwatersrand Basin occurred long after the sediments had been deposited. Transformation of organic matter (in this case Type I, algal-dominated kerogen made up largely of aliphatic chains) in the Witwatersrand Basin would have followed a normal evolution through diagenetic and catagenic stages where subsidence rates and burial of the sequence must have been moderate to low. Type I kerogens would have adjusted continuously to the increasing pressures and temperatures by progressive elimination of functional groups and scission, to form a variety of low- to medium-molecular weight hydrocarbons, in addition to CO_2 and H_2O. Maximum production of mobile (liquid and gaseous) hydrocarbons appears to have taken place up to 400 Ma after the sediments had been laid down, as suggested by the U-Pb isotopic evidence. Polymerization and condensation of these mobile hydrocarbons would then have been induced by ionizing radiation in the proximity of uranium phases, which created the presence of free-radicals and enhanced cross-linking reactions.

In peraluminous granites adjacent to the Witwatersrand Basin hydrocarbon-bearing brines originating from within the basin during the period of maximum liquid hydrocarbon expulsion would have percolated along the sediment-basement interface into pre-existing fractures, themselves possibly the locus for pre-existing hydrothermal fluid flow (Figure 7). Since most of the peraluminous granites adjacent to the Witwatersrand contain abundant accessory uraninite and/or uranothorite (Robb *et al.*, 1990), small quantities of hydrocarbons would have agglutinated around and replaced these phases by radiolytic polymerization. The volumes of hydrocarbon fixed in these granites would have been determined by the amount of accessory high-U phases present in the rock, and since the ratio of kerogen to uraninite/uranothorite is ≤ 1 the combined effects (including thermal) of polymerization would have been severe, thereby giving rise to a more organized hydrocarbon structure than that present in the conglomeratic reefs (Figure 7). It is pertinent to note that bituminous hydrocarbon

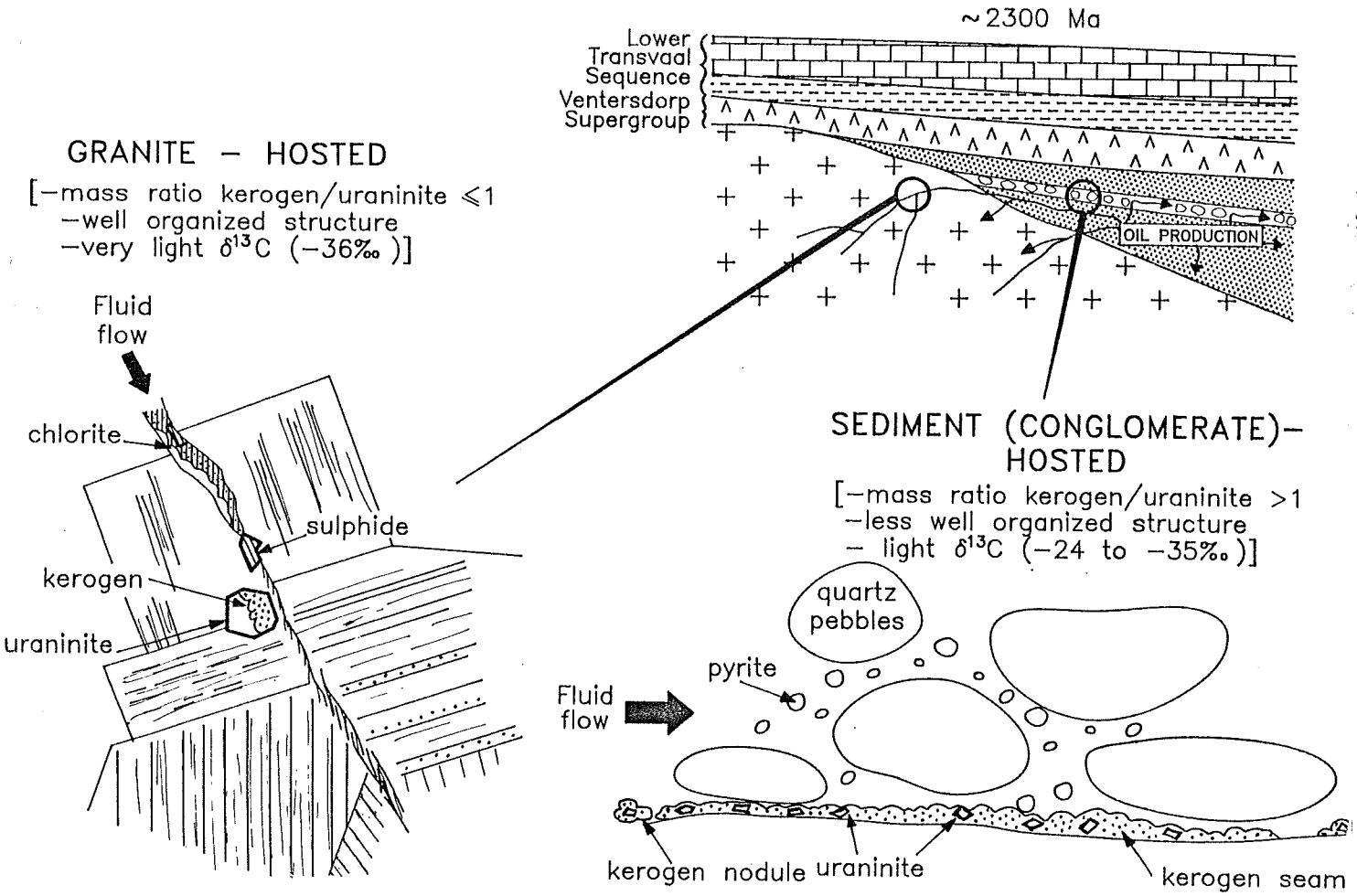

Figure 7: Model relating hydrocarbon fixation in peraluminous granites and Witwatersrand conglomerates to a single event of oil production some time (~ 2300 Ma ago) after deposition of the sediments. Raman structural characteristics are related to relative proportions of kerogen and uraninite/uranothorite in the respective host rocks. Hydrocarbons that have migrated further from their source will be characterized by lighter $\delta^{13}C$ values.

rims have been reported around monazite grains from heavy mineral lags in Permo-Triassic arenites of Western Australia (Rasmussen *et al.*, 1989). Fixation of the hydrocarbons around monazite has been attributed here to radiolytic polymerization since similar rims were not observed around low U-Th zircon grains in the same lags. A similiar hypothesis has also recently been suggested for the formation of uranium-rich bitumens in the Cigar Lake deposit of northern Saskatchewan (Landais, 1992).

In the Witwatersrand conglomerates the processes of hydrocarbon fixation would have been similar except that the volumes of detrital uraninite concentrated during placer formation are far greater than those present as accessory phases in granites (Figure 7). Consequently, significant quantities of hydrocarbon became fixed in and around lags of uraninite within the conglomerates, resulting in the formation of seams of carbonaceous matter often, but not always, along the base of the conglomeratic unit. Since the volume of kerogen relative to

uraninite is > 1 the effects of polymerization diminish away from individual uraninite grains within the kerogen seam. This results in considerable variations of the composition and structural state of the kerogen (Landais *et al.*, 1990a; in prep.).

The presence of nodular kerogen in peraluminous granites adjacent to the Witwatersrand Basin has major implications for the origin of carbonaceous matter in the basin. Similarities in composition, maturation, U-Pb and C isotopic signatures, as well as the intimate association with uraninite and the late paragenesis, suggest that the processes of hydrocarbon migration and fixation, which are *ipso facto* epigenetic in granitic host rocks, must also have applied within the sediments from which the organic matter was derived. Kerogen seams and nodules within Witwatersrand conglomerates, which are paragenetically late and also associated with detrital uraninite lags, probably formed, therefore, as a consequence of a discrete period of oil or gas production, the migrated products of which were fixed by radiolytic polymerization. This implies that the Witwatersrand kerogen, although ultimately derived from the decay of algal material, is unlikely, *in its present position,* to represent the fossilized *in situ* residue of algal mats.

ACKNOWLEDGEMENTS

The authors acknowledge the FRD for financial support, and Derek de Bruiyn, Department of Geology, University of the Orange Free State, Bloemfontein, for the uranothorite microprobe analysis. Pat King, Janet Long and Lyn Whitfield are thanked for secretarial and drafting assistance.

REFERENCES

Allsopp, H.L., Evans, I.B., Giusti, L., Hallbauer, D.K., Jones, M.Q.W. and **Welke, H.J.** (1986). U-Pb dating and isotopic characterization of carbonaceous components of the Witwatersrand reefs. Ext. Abstr. Geocongress '86, Johannesburg, 85-88.

Armstrong, R.A., Compston, W., Retief, E.A., Williams, I.S. and **Welke, H.J.** (1991). Zircon ion-microprobe studies bearing on the age of evolution of the Witwatersrand Triad. Precambrian Res., **53**, 243-266.

Burger, A.J. and **Coertze, F.J.** (1974). Age determinations - April 1972 to March 1974. Annals Geol. Surv. S. Afr., **10**, 135 -141.

Eakin, P.A. (1989). Isotopic and petrographic studies of uraniferous hydrocarbons from around the Irish Sea Basin. J. Geol. Soc. Lond., **146**, 663-673.

Eglington, B.M. and **Harmer, R.E.** (1991). Geodate: A program for the processing and regression of isotope data using IBM compatible micro-computers. CSIR Manual EMA-H 9101, 57pp.

Förster, O. (1989). Geochemische und isotopengeochemische Untersuchungen an Kohle und Goldfuhrenden Konglomeraten des Proterozoikums (Central Rand Group, South Africa). Ph.D. thesis (unpubl.), Univ. Munich, 149pp.

Fryer, B.J. and **Taylor, R.P.** (1987). Rare earth element distributions in uraninites: implications for ore genesis. Chem. Geol., **63**, 101-108.

Gellatly, D.C. (1966). Graphite in natural and experimental carbonate systems. Min. Mag., **35**, 963-970.

Hallbauer, D.K. (1975). The plant origin of the Witwatersrand carbon. Mineral. Sci. Eng. **7**, 111-131.

Hallbauer, D.K. (1984). Archaean granitic sources for the detrital mineral assemblage in Witwatersrand conglomerates. Ext. Abstr., Geocongress '84, Potchefstroom, 53-56.

Hallbauer, D.K. (1986). The mineralogy and geochemistry of Witwatersrand pyrite, gold, uranium and carbonaceous matter. *In:* Anhauesser, C.R. and Maske, S. (Eds.), Mineral Deposits of Southern Africa. I, Geol. Soc. S. Afr., 731-752.

Hallbauer, D.K. (1991). Trace element contents and isotopic geochemistry of Witwatersrand carbonaceous matter. Abstr. Symp. on Carbon in Witwatersrand Reefs, Geol. Soc. S. Afr., Carletonville, 103-104.

Hallbauer, D.K., Klemd, R. and **Von Gehlen, K.** (1986). A provenance model for the Witwatersrand gold and uranium mineralization and its implications in the recognition of gold distribution patterns in reefs. Ext. Abstr. Geocongress '86, Johannesburg, 133-137.

Hoefs, J. and **Schidlowski, M.** (1967). Carbon isotope compositions of carbonaceous matter from the Precambrian of the Witwatersrand System. Science, **155**, 1096-1097.

Jahn, B-M., Bertrand-Safarti, J., Morin, N. and **Macé, J.** (1990). Direct dating of stromatolitic carbonates from the Schidtsdrift Formation (Transvaal Dolomites), South Africa, with implications on the age of the Ventersdorp Supergroup. Geology, **18**, 1211 - 1214.

Klemd, R. and **Hallbauer, D.K.** (1987). Hydrothermally altered peraluminous Archaean granites as a provenance model for Witwatersrand sediments. Mineral. Deposita, **22**, 227-235.

Landais, P. (1992). Bitumens in uranium deposits. *In:* Parnell, J., Landais, P. and Kucha, H. (Eds.), Bitumens in Ore Deposits. Springer-Verlag, in press.

Landais, P., Dubessy, J., Poty, B. and **Robb, L.J.** (1990a). Three examples illustrating the analysis of organic matter associated with uranium ores. Org. Geochem., **16**, 601-608.

Landais, P., Dubessy, J., Robb, L.J. and **Nouel, C.** (1990b). Preliminary chemical analyses and Raman spectroscopy on selected samples of Witwatersrand kerogen. Inform. Circ. Econ. Geol. Res. Unit, Univ. Witwatersrand, Johannesburg, **222**, 8pp.

Nagy, B., Gauthier-Lafaye, F., Holliger, P., Davis, D.W., Mossman, D.J., Leventhal, J.S., Rigali, M.J. and **Parnell, J.** (1991). Organic matter and containment of uranium and fissiogenic isotopes at the Oklo natural reactors. Nature, **354**, 472-475.

Rasmussen, B., Glover, J.E. and **Alexander, R.** (1989). Hydrocarbon rims on monazite in Permian-Triassic arenites, northern Perth Basin, Western Australia: pointers to the former presence of oil. Geology, **17**, 115-118.

Robb, L.J. and **Meyer, F.M.** (1987). The nature of the Archaean basement in the hinterland of the Witwatersrand Basin: I. The Rand anticline between Randfontein and Rysmierbult. S. Afr. J. Geol., **90**(1), 44-63.

Robb, L.J. and **Meyer, F.M.** (1990). The nature of the Witwatersrand hinterland: conjectures on the source area problem. Econ. Geol., **85**, 511 - 536.

Robb, L.J., Meyer, F.M., Ferraz, M.F. and **Drennan, G.R.** (1990). The distribution of radioelements in Archaean granites of the Kaapvaal Craton, with implications for the force of uranium in the Witwatersrand Basin. S. Afr. J. Geol., **93**(1), 5-40.

Robb, L.J., Davis, D.W., Kamo, S.L. and **Meyer, F.M.** (1992). Ages of altered granites adjoining the Witwatersrand Basin with implications for the source of gold and uranium. Nature, **357**, 677-680.

Rochdi, A. and **Landais, P.** (1991). Transmission micro-infrared spectroscopy: a tool for micro-scale characterization of coal. Fuel, **70**, 367-371.

Roscoe, S.M. (1969). Huronian rocks and uraniferous conglomerates in the Canadian Shield. Geol. Surv. Canada Paper **68-40**, 205pp.

Rumble, D., Duke, E.F. and **Hoering, T.L.** (1986). Hydrothermal graphite in New Hampshire: Evidence of carbon mobility during regional metamorphism. Geology, **14**, 452-455.

Schidlowski, M. (1981). Uraniferous constituents of the Witwatersrand conglomerates: ore-microscopic observations and implications for Witwatersrand metallogeny. *In:* Armstrong, F. (Ed.), Genesis of Uranium- and Gold-bearing Precambrian Quartz-pebble Conglomerates. U.S. Geol. Surv. Prof. Pap., **1161**, 1-29.

Tissot, B.P. and **Welte, D.H.** (1978). Petroleum Formation and Occurrence. Springer - Verlag, New York, 699pp.

Wallmach, T. and **Meyer, F.M.** (1990). A petrogenetic grid for metamorphosed aluminous shales. S. Afr. J. Geol., **93**(1), 93-102.

Wang, A., Dhamelincourt, P., Dubessy, J., Guerard, D., Landais, P. and **Lelaurain, M.** (1989). Characterization of graphite alteration in a uranium deposit by micro-Raman spectroscopy, X-ray diffraction, transmission electron microscopy and scanning electron microscopy. Carbon, **27**, 209-218.

Waples D. (1982). Organic Geochemistry for Exploration Geologists. Int. Human Res. Dev. Corp., Boston, 233pp.

Zumberge, J.E., Sigleo, A.C. and **Nagy, B.** (1978). Molecular and elemental analysis of carbonaceous matter in the gold and uranium bearing Vaal Reef carbon seams, Witwatersrand sequence. Mineral. Sci. Eng., **10**, 223-246.

_____oOo_____